Ocean Dynamics (2024) 74:321–334
https://doi.org/10.1007/s10236-024-01606-x

Pathways of surface oceanic water intrusion into the Amazon Continental Shelf

Pedro Paulo de Freitas[1] · Mauro Cirano[2] · Carlos Eduardo Peres Teixeira[3] · Martinho Marta-Almeida[4] · Francisco Flávio de Brito Borges[1] · Camilo Andrés Guerrero-Martin[1] · Vando José Costa Gomes[1]

Received: 6 June 2023 / Accepted: 18 February 2024 / Published online: 28 February 2024

Abstract

The Amazon Continental Shelf (ACS) is a shallow region (< 100 m), with a maximum width of 330 km, which encloses the northern portion of the Brazilian continental shelf and has great ecological and climatic importance on a global scale. Although important scientific efforts have been made to understand the hydrodynamics of the ACS and the dispersion of the Amazon River plume, there are still few studies that address surface oceanic water intrusion into the ACS. This study describes the existence of preferential surface oceanic water intrusion pathways into the ACS along 3 sectors: Maranhão (MA shelf), Pará (PA shelf) and Amapá (AP shelf). The analysis is based on: (i) 306 surface drifter trajectories along 1344 km of the ACS (provided by the Global Drifter Program) and (ii) 20 years of Lagrangian simulations (with Parcels model forced by currents from the reanalysis GLORYS). The results show that the MA shelf sector is the main pathway for surface oceanic water intrusions into the ACS, corresponding to 56% of the intrusions, followed by PA shelf (43%) and AP shelf (1%). During the austral summer, intrusions occur with a higher frequency in PA and AP shelf. The MA shelf shows weak seasonality in the intrusions. The temporal variability of particle intrusion rates into the ACS is directly related to the variability of the trade winds, and the meso-scale circulation associated with the North Brazil Current and the North Equatorial Countercurrent.

Keywords Cross-shelf exchange · Global drifter program · Lagrangian modeling · Ocean Forecasting and analysis system

This article is part of the Topical Collection on the Coastal Ocean and Shelf Seas Task Team (COSS-TT) meeting, Montreal, Canada, May 2-4, 2023.

✉ Pedro Paulo de Freitas
pedropaulo.oceano@gmail.com

Mauro Cirano
mauro.cirano@igeo.ufrj.br

Carlos Eduardo Peres Teixeira
carlos.teixeira@ufc.br

Martinho Marta-Almeida
m.martalmeida@gmail.com

Francisco Flávio de Brito Borges
fl4vioborges@gmail.com; vandogomes@ufpa.br

Camilo Andrés Guerrero-Martin
camiloguerrero@ufpa.br

[1] Faculdade de Engenharia, Universidade Federal do Pará (UFPA), Salinópolis, Pará, Brazil

[2] Departamento de Meteorologia, Instituto de Geociências, Universidade Federal do Rio de Janeiro (UFRJ), Rio de Janeiro, Brazil

[3] Instituto de Ciências do Mar, Labomar, Universidade Federal do Ceará (UFC), Fortaleza, Brazil

[4] Centro Oceanográfico de A Coruña, Instituto Español de Oceanografia (IEO-CSIC), A Coruña, Spain

1 Introduction

The continental shelves are shallow regions (< 500 m), highly dynamic and with great relevance for the: (i) primary productivity of the oceans, (ii) biogeochemical cycles, (iii) sediment transport and deposition at the continental/ocean interface, and (iv) development of strategic economic activities. The Amazon Continental Shelf (ACS) is a wide shallow region (< 100 m), which encloses the northern portion of the Brazilian continental shelf and is delimited between 2°S and 4°N (Fig. 1) (Nittrouer and DeMaster, 1986; Castro et al. 2006). The ACS is located on a continental margin with great potential for oil exploration (Almeida et al. 2020; Cruz et al. 2021) and fishing resources (Cruz et al. 2013; Araújo et al. 2022), and has great ecological and climatic importance on a global scale (Moura et al. 2016; Francini-Filho et al. 2018; Lavagnino et al. 2020; Louchard et al. 2021).

ACS hydrodynamics are highly energetic and modulated by river discharge, tides, trade winds and the North Brazil Current (NBC) (Geyer et al. 1996; Nittrouer and DeMaster, 1996; Aguiar et al. 2022). The discharge of the Amazon River corresponds to roughly 18% of the global river discharge and plays a role in modulating the physical and sedimentological characteristics of the ACS (Nittrouer and DeMaster 1986; Lentz and Limeburner 1995; Oliveira et al. 2018). Tides on the ACS are dominated by the lunar semidiurnal component M_2, with sea level variations at the coast greater than 5 m and tidal currents of up to 2 m s^{-1} (Beardsley et al. 1995; Geyer et al. 1996), which play a crucial role in vertical mixing and in the generation of cross-slope mass fluxes (Fontes et al. 2008; Prestes et al. 2018).

The trade winds are an important forcing mechanism for the surface circulation of the ACS and adjacent oceanic region. The seasonal variation of the latitudinal position of the Intertropical Convergence Zone (ITCZ) results in changes in the intensity and predominant direction of the trade winds on the Brazilian equatorial margin. During the austral winter the ITCZ shifts to latitudes north of the equator (Adam et al. 2016; Schneider et al. 2014) and the southeast trade winds are dominant, forcing stronger alongshore currents (Castro et al. 2006). While during the austral summer, the northeast trade winds are predominant, and can generate cross-slope flows (Lentz 1995; Lentz and Limeburner 1995).

The NBC is an important northwestward boundary current feature of the ACS hydrodynamics, presenting an average position between the outer shelf (100 m isobath) and continental slope (1000 m isobath) (Johns et al. 1998). The origin of the NBC is associated with the combination of flows from the North Brazil Undercurrent (NBUC) and the central branch of the South Equatorial Current (cSEC) at approximately 35°W, and between 5°S and the Equator (Silveira et al. 1994; Schott et al. 2005). Adjacent to the ACS, the NBC presents average speeds of 0.9 m s^{-1} a core at about 50 m depth (Bourlès et al. 1999) and a vertical velocity structure that extends throughout the upper 1000 m of the water column (Schott et al. 1998; Stramma et al. 2005). Studies performed on the ACS reveal that the NBC modulates the intensity and direction of the alongshore currents at the outer shelf (Prestes et al. 2018) and advects low salinity waters from the Amazon River towards the Caribbean sea and the NBC retroflection region (Aguiar et al. 2022). Therefore, the variability of NBC plays an important role in

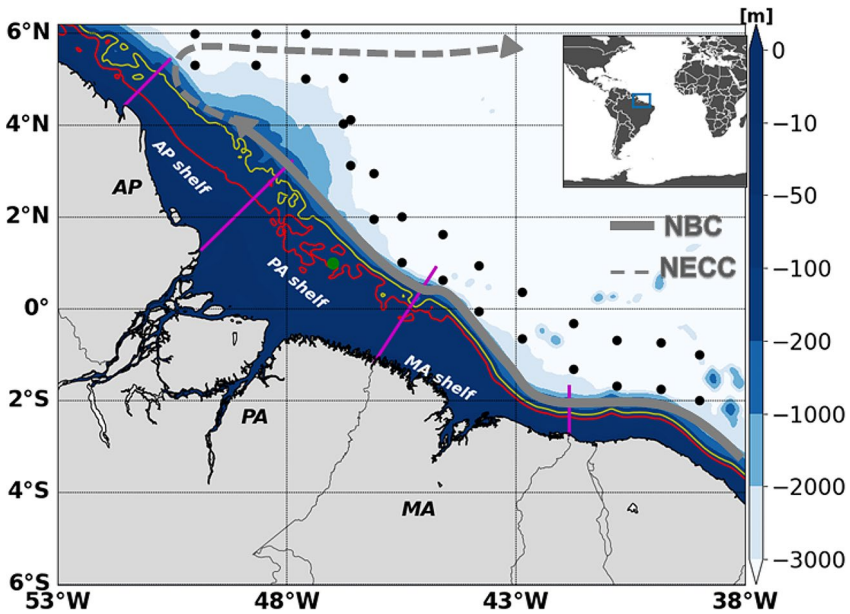

Fig. 1 Lagrangian model domain and bathymetry of the Amazon Continental Shelf (shaded), including Maranhão shelf [MA], Pará shelf [PA] and Amapá shelf [AP]. The magenta line indicates the boundaries between the Amazon Continental Shelf sectors. The black dots indicate the positions at which particles were released at the surface in the simulations, on the isobaths of 2000 and 3000 m. The green dot indicates the location where GLORYS SSH was validated against AVISO. The inset indicates the search area for drifters and the analysis area of 20 years of high resolution numerical reanalysis results (GLORYS) provided by the Copernicus Marine Environment Monitoring Service (CMEMS). The continuous grey line schematically indicates the position of the NBC, followed by a dotted line indicating the North Equatorial Counter Current (NECC)

the generation of water fluxes between the oceanic region and the ACS.

Mass exchange between the oceanic region and the continental shelf can be generated by different physical processes and is an important scientific issue in coastal physical oceanography (Huthnance 1995; Brink 2016). Studies around the world show that these exchanges may occur due to the influence of: (i) boundary currents and associated mesoscale activity (Malan et al. 2020; Guerrero et al. 2020), (ii) wind variability (Matano et al. 2014; Combes et al. 2021) and/or (iii) a combination of different physical mechanisms, such as wind, boundary currents, internal waves and tides (Zhou et al. 2015; Huang et al. 2021; Huthnance et al. 2022; Berden et al. 2022).

Most of the studies performed on the ACS related to mass exchange between the shelf and the ocean address the dispersion of the Amazon River plume in order to characterize the importance of: seasonality in Amazon River discharge, tides, trade winds and the NBC (Lentz 1995; Lentz and Limeburner 1995; Fontes et al. 2008; Coles et al. 2013; Aguiar et al. 2022). Molinas et al. (2020) demonstrate, using numerical modeling, that the internal tides also play an important role in the cross-shelf transport of fine sediments at the Amazon shelf break region. Finally, based on 3 months of historical hydrographic data, Silva et al. (2005) show the occurrence of oceanic water intrusion into the continental shelf driven by the adjacent oceanic circulation.

Despite the important scientific contributions made in understanding the ACS hydrodynamics, there are various knowledge gaps associated with the intrusion of oceanic water on the continental shelf, in terms of the identification of preferential paths, temporal variability of the intrusions and forcing mechanisms. The intrusion of oceanic water into the continental shelf modulates the hydrodynamic variability of these regions and can play an important role in the dynamics of fishery resources, nutrients and pollutants (Cruz et al. 2013; Garcia et al. 2020).

A recent oil spill off the Brazilian coast in 2019/2020 (Soares et al. 2020), for example, showed how fundamental it is to understand the processes that lead to mass flows between the adjacent ocean and the associated continental shelf. In this event, several locations along the Brazilian coast were impacted by the oil, including regions of ecological relevance such as estuaries, mangroves, beaches, tidal flats and coral reefs (Magris and Giarrizzo 2020). Lessa et al. (2021) identified the driving mechanisms of the oil into the Brazilian northeast shelf, however these driving mechanisms are unknown to the ACS.

Thus, based on surface drifter trajectories along 1344 km of the ACS provided by the Global Drifter Program (GDP), 20 years of high resolution numerical reanalysis results (GLORYS) provided by the Copernicus Marine Environment Monitoring Service (CMEMS), and Lagrangian simulations, this study aims to characterize the occurrence of surface oceanic water intrusion into the ACS. This objective involves: (i) the identification of preferential pathways of oceanic surface water intrusion in 3 sectors of the ACS (Maranhão – MA shelf, Pará – PA shelf and Amapá – AP shelf), (ii) the characterization of their seasonal variability and (iii) their correlation with the temporal variability of the trade winds and the NBC.

2 Data and methods

2.1 Observational data

This study used hourly trajectory and velocity data collected by satellite-tracked surface drifting buoys (drifters) of the NOAA GDP (https://www.aoml.noaa.gov/phod/gdp), a valuable dataset for the study of oceanic processes (Elipot et al. 2016, 2022). Drifters were selected between 2001 and 2020 in the area between 40°W – 53°W and 6°S – 6°N (shown in Fig. 1), accounting for a total of 306 drifters. The selected area encloses the entire ACS and adjacent oceanic region.

Figure 2 presents the temporal distribution of the number of observations of drifters in the study area, showing that the number of trajectories available for analysis is temporally heterogeneous both in terms of months and in terms of years. For this reason, this study adopted a complementary methodology to include numerical modeling, in order to fill temporal and spatial gaps of the observations.

2.2 Ocean reanalysis data

This study is based on the results from the Global Ocean Reanalysis (GLORYS), which is an eddy resolving (1/12° horizontal resolution) global ocean simulation implemented by Copernicus Marine Environment Monitoring Service (CMEMS) (https://data.marine.copernicus.eu/product/GLOBAL_MULTIYEAR_PHY_001_030/description). The GLORYS is based on the NEMO platform (Madec and the NEMO Team, 2008), with most of the reanalysis components coming from the current real-time global CMEMS high-resolution forecasting system (PSY4V3) (Lellouche et al. 2018), forced at the surface by atmospheric fields from the ERA5 reanalysis (Dee et al. 2011), without tides and with assimilation of altimetric sea level anomaly data along track, sea surface temperature measured by satellites and vertical profiles of temperature and salinity (Jean-Michel et al. 2021).

20 years (2001–2020) of daily surface velocity fields from the GLORYS for the area between 53°W – 30°W

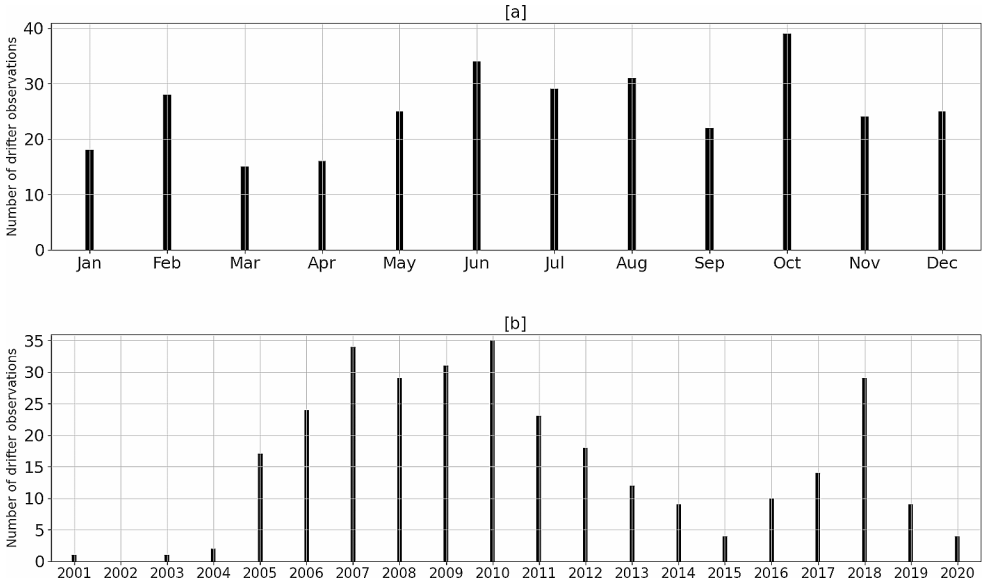

Fig. 2 Temporal occurrence of the 306 drifters analyzed in the region of interest (55°W – 40°W, 6°S and 6°N) from 2001 to 2020. **a** Accumulated number of drifter observations per month during the whole period. **b** Number of drifter observations per year

and 6°S – 6°N (Fig. 1) have been used in order to force the Lagrangian model and to analyze the seasonal variability of the circulation.

2.3 Altimetry data

This study used a 20-year daily time series of sea surface height data from AVISO (https://www.aviso.altimetry.fr/en/data/data-access.html) on the ACS(47°W, 1°N) to validate the interannual variability of the GLORYS reanalysis circulation.

2.4 Lagrangian modeling

Lagrangian modeling was used to identify preferential pathways of oceanic surface water intrusion into the ACS and to investigate how the space-time variability of the NBC circulation affects these intrusions. This study used the Ocean Parcels toolbox (Parcels v2.2.0) (Delandmeter and Sebille 2019), which has been frequently used for studies that investigate trajectories in ocean circulation (Iskandar et al. 2022; Chen 2023; Silveira et al. 2023).

The Lagrangian experiment was carried out using 20 years (2001–2020) of daily surface velocity fields (u and v) from the GLORYS and daily releases of 2 particles at 14 pairs of points were done (Fig. 1), accounting for a total of 204,512 released particles. The particle advection was performed with a time step of 1 day, using the Runge-Kutta4 scheme, and without horizontal diffusion. The trajectory of each particle was followed individually, in order to identify the occurrence of intrusion, and to characterize the location and date of the occurrence.

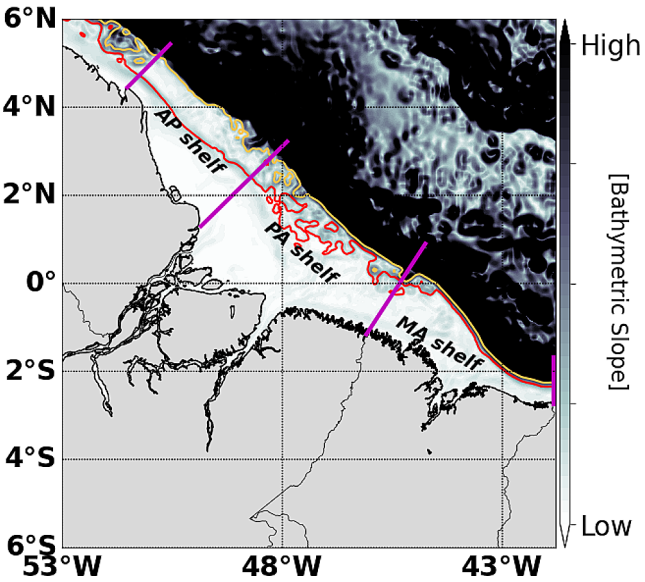

Fig. 3 Bathymetric slope of the study area (shaded) calculated from ETOPO 1. The 50 m isobath is highlighted (red), indicating the criterion for intrusion into the ACS. The 100 m isobath is highlighted (yellow), indicating the approximate position of the shelf break

2.5 Analysis

The average depth of the Amazon shelf break is defined in the scientific literature as being at the 100 m isobath (Nittrouer and DeMaster, 1986), and can be up to 300 m in the AP Shelf sector (Lavagnino et al. 2020). Considering these values, the bathymetric slope of the ACS and adjacent oceanic region was calculated using the ETOPO1 (https://www.ncei.noaa.gov/products/etopo-global-relief-model) bathymetry (Fig. 3) in order to illustrate that the 100 m isobath (yellow line) is a good approximation for the transition between the shelf (lower bathymetric gradient) and the continental

slope (higher bathymetric gradient). Considering also that the NBC flows close to the outer shelf (Schott et al. 1995), this study adopted as a criterion for intrusion into the ACS the detection of drifters and/or particles crossing the 50 m isobath (Fig. 3, red line) and remaining in equal or shallower depths for at least 1 day.

A total of 306 drifters were detected in the study area, of which 122 showed trajectories of intrusion into the ACS. Velocity data collected from drifters following trajectories along the continental shelf were used to validate the GLORYS model.

The temporal variability analysis of particle intrusion rates was carried out for the traditional 3 month austral seasons: summer, autumn, winter and spring. These periods are justified due to the variability of the trade winds associated with the migration of the ITCZ and the variability of the NBC retroflection and transport, which are important physical mechanisms of the hydrodynamic variability of the region (Servain et al. 1999; Garzoli et al. 2004).

3 Results

The results are organized into two sections, which address: (i) validation of the GLORYS ocean reanalysis and (ii) characterization of the preferential pathways of surface oceanic water intrusion into three sectors of the ACS.

3.1 Model validation

Based on velocity and trajectory measurements of GDP drifters, and sea surface height above geoid provided by AVISO, we validated the GLORYS circulation in the region, used to force the Lagrangian model.

Velocity data from the entire track of 122 GDP drifters with intrusion path into the ACS (Sect. 2.5) were compared with the reanalysis velocities using a least squares fitting for each velocity component (Fig. 4[a, b]). Velocity data were low-pass filtered using 72 h cut-off in order to eliminate the tidal and other high frequency signals. The GDP data were interpolated onto the daily time domain of GLORYS. The comparison between the data and model velocity series (not shown), and the values of r^2 (0.7 and 0.6) from the least squares fitting, show that the model effectively captures the variability of currents within the region.

Two experiments were carried out with the Lagrangian model in order to illustrate the representability of the circulation in the study area by GLORYS and the trajectories generated by the Lagrangian modeling. The experiments performed particle releases at the same time and initial position of a GDP drifter. Particle trajectories (Fig. 4 [c, d]) illustrate that the reanalysis surface velocity field represents well the circulation of the region, leading to simulated trajectories in strong agreement with the observed ones. These two specific drifter examples were chosen to highlight two typical scenarios of the exchange processes between the oceanic region and the continental shelf in the study area. These scenarios specifically address: (i) the influence of the oceanic mesoscale and (ii) the direct path of drifter intrusion into the ACS.

Based on 20 years trajectories of the GDP drifters and the particles from the Lagrangian modeling carried out during the period between 2001 and 2020, released at 39°W, 2°S, and 39°W, 1°S (first pair in Fig. 1), we estimated its permanence time on the ACS after the intrusion for four time bands: i)1–30 days, ii) 31–60 days, iii) 61–90 days and iv) > 90 days. The histogram in Fig. 5 reveals that trajectories of the GDP data and Lagrangian modeling present the time band between 1 and 30 days as the most frequent residence time, followed by the bands between 31 and 60 days and 61–90 days. Particles released in the Lagrangian simulations exhibit permanence time on the ACS similar to that observed in the GDP drifters, which reinforces that the GLORYS surface velocity field represents well the circulation variability on the ACS.

The interannual variability of surface circulation of the reanalysis was analyzed based on a comparison between the daily series of sea surface height above geoid (SSH) of the model and the AVISO data at a representative location on the ACS (47°W, 1°N in Fig. 1), during the period 2001 to 2020. The comparison (Fig. 6) shows GLORYS reproduces well the high and low frequency variability of the SSH measured by AVISO despite the fact that it does not represent some minimum and maximum peaks of SSH with the same amplitude.

3.2 Preferential pathways

3.2.1 *Observations*

The analysis of the trajectories of the GDP drifters allowed for the first time to map pathways of surface oceanic water intrusion into the ACS. Figure 7 illustrates the positions where the drifters crossed the 50 m isobath and shows that the MA shelf is the sector where most observations of intrusion occurred, followed by the PA shelf. From a total of 306 drifters selected in the study region, 122 entered into the ACS, and of these, 76% entered through the MA shelf sector, 24% through the PA shelf sector and no drifter entered through the AP shelf (Fig. 8 [a]).

The analysis of the seasonality of drifter intrusions into the ACS (Fig. 8 [b]) shows that intrusions in the MA shelf are 4-6% more frequent during the austral winter season (29%) than in the spring (25%), summer (22%) and autumn (24%).

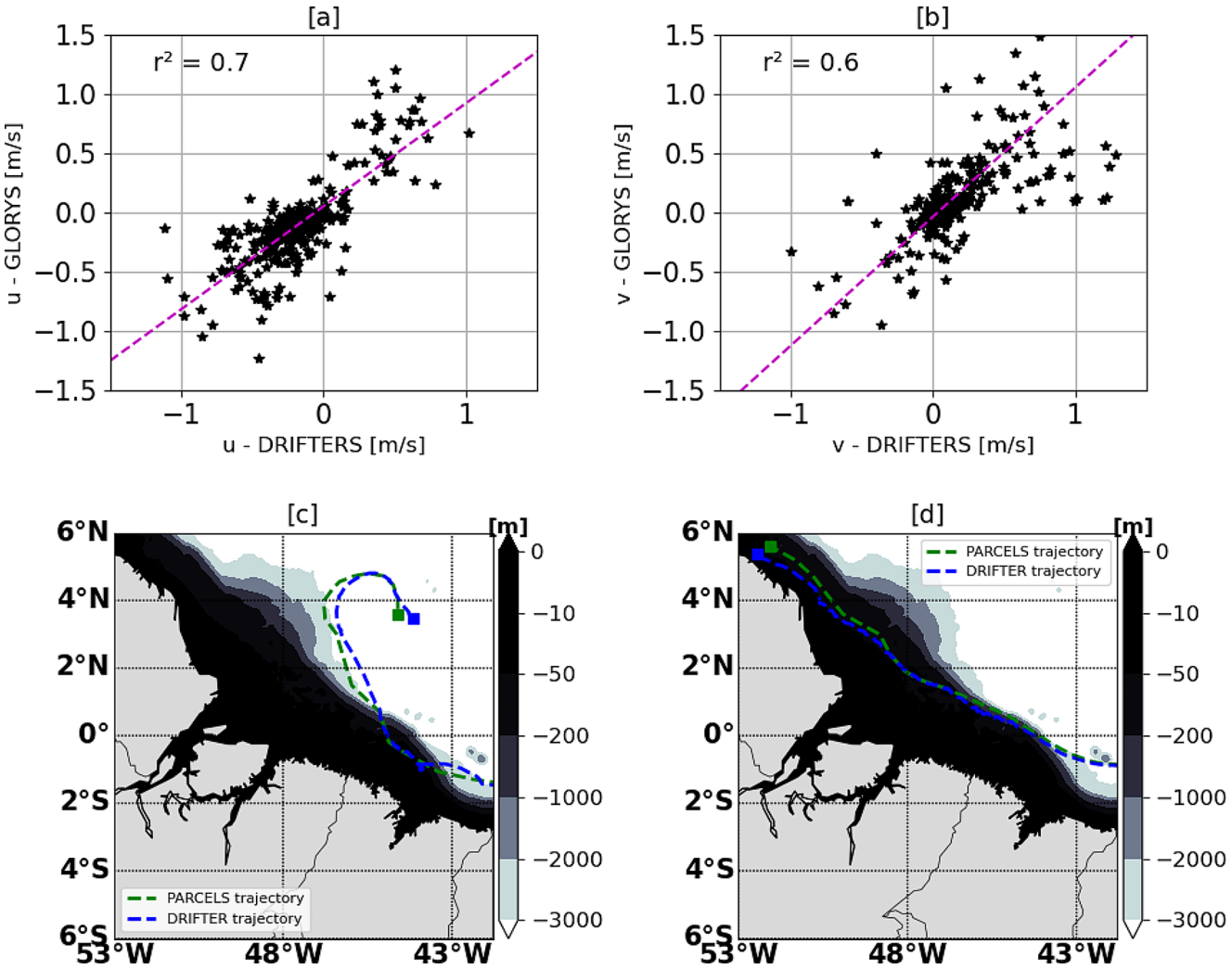

Fig. 4 [**a**] and [**b**] Scatters of the zonal (u) and meridional(v) velocity components, respectively, measured by GDP drifters that traversed onto the Amazon Continental Shelf in the period between 2001 and 2020 and the co-located GLORYS surface velocity components. The magenta line in panels a and b indicates a least squares fitting between the data and model series. **c** and **d** illustrate comparisons between the trajectory of a GDP drifter (blue line) and the trajectory simulated by Parcels using the surface velocity fields of GLORYS during the period between 2008/06/01–2008/06/20 (**c**) and between 2011/12/17–2012/01/11 (**d**), respectively

In the PA shelf sector, more intrusions were observed during austral winter (38%) than in spring (21%), summer (24%) and autumn (17%). The results of the analysis may not be robust given the small sample size, particularly for the PA shelf(Fig. 2 [a]). In order to fill in these data limitations, we present the results obtained from the Lagrangian experiment in the next section.

3.2.2 Lagrangian modeling

The analysis of the trajectories of the particles released in the Lagrangian experiment over 20 years (2001–2020) allowed for a robust statistical characterization of the intrusions into the three sectors of the ACS. Of the total of 204,512 particles released, 19% entered the ACS, and of this fraction, 56% penetrated the MA shelf, 43% the PA shelf, and 1% the AP shelf. (Fig. 9, [a]). This spatial differentiation of intrusion into the ACS is similar to that observed in the trajectories of the GDP drifters, reinforcing that the GLORYS accurately represents the hydrodynamics of the oceanic region responsible for the surface flows into the ACS. However, it must be emphasized that the spatial separation in the intrusion rates is more pronounced in the GDP drifters observations.

The Lagrangian results (Fig. 9, [b]) show weak seasonality in intrusion rates in the MA shelf sector, with higher values during the austral spring (28%) and a minimum in the winter (21%). Although seasonal signal is weak, the good agreement between the model and drifter seasonality in the MA shelf intrusions is encouraging, as this is the region with higher availability of drifter data. On the other hand, the

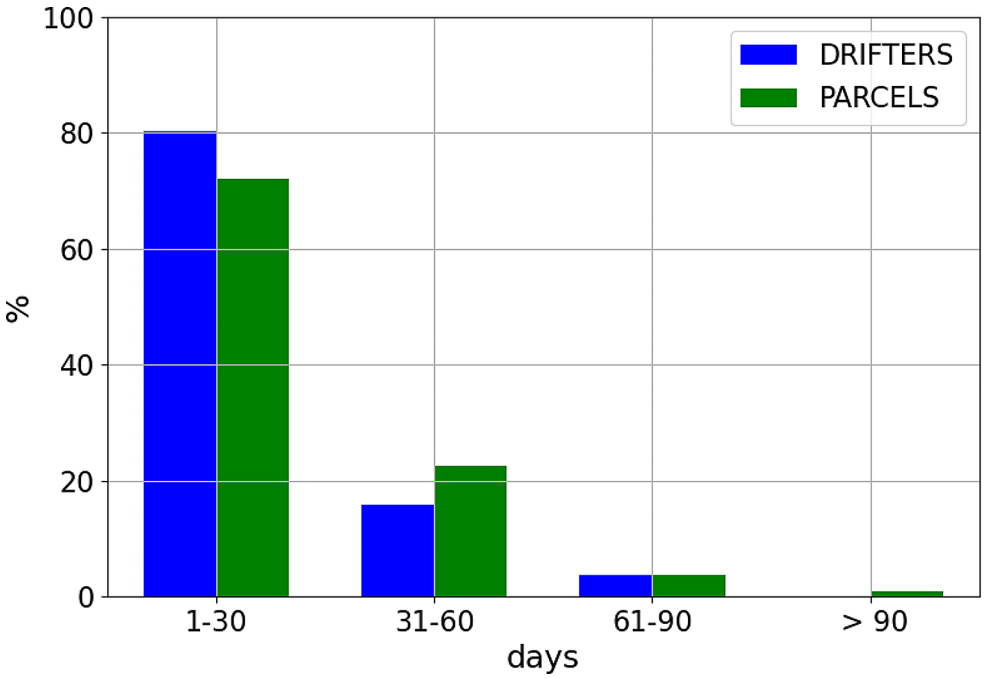

Fig. 5 Histogram of the permanence time on the Amazon Continental Shelf of drifters from GDP (blue) and particles (green) released at 39°W, 2°S and 39°W, 1°S during Lagrangian modeling (2001–2020) for four time bands: (i) 1–30 days, (ii) 31–60 days, (iii) 61–90 days and (iv) > 90 days

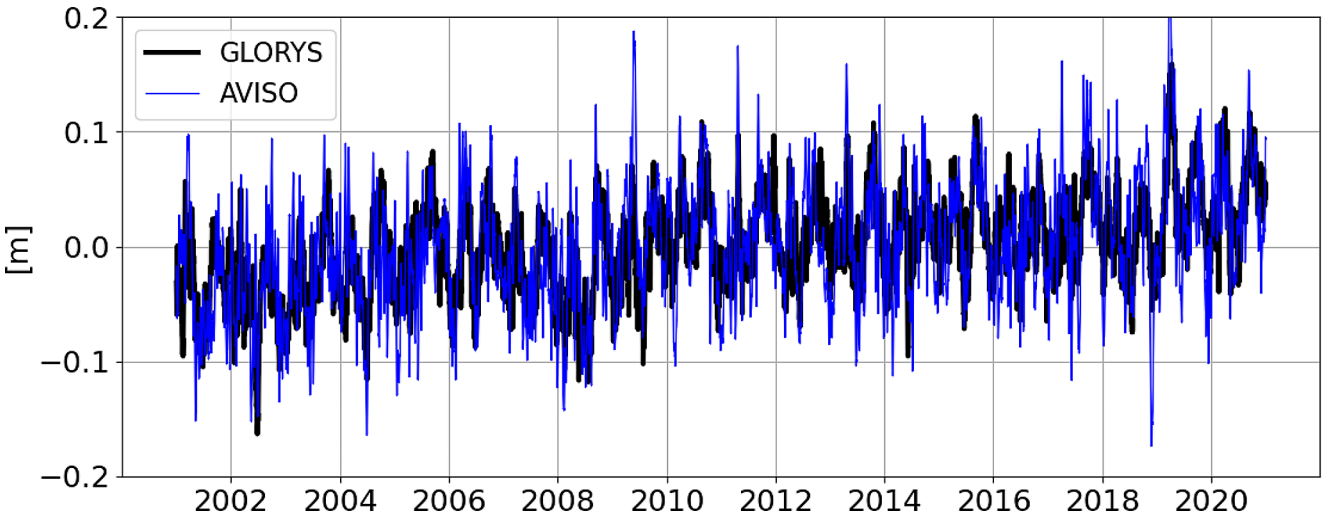

Fig. 6 A comparison between the daily series of sea surface height above the geoid (SSH) of the model (black line) and AVISO (blue line) on the Amazon Continental Shelf (47°W, 1°N). The correlation between the series is 0.6, and the RMSE is 0.04 m

PA and AP shelf sectors exhibit pronounced seasonality in intrusion rates. The PA shelf shows higher values in spring (31%) and summer (40%) compared to autumn (14%) and winter (15%). While there is lack of agreement between the model and drifter seasonality in the PA shelf intrusions, it should be noted that the sparsity of drifter intrusions (29 onto the PA shelf) implies that the drifter seasonal statistics may not be robust. The AP shelf exhibits the most significant seasonality among all sectors, with an intrusion rate of 96% during the summer, 4% in the autumn, and no intrusion during the winter and spring. The lack of intrusion in the AP shelf sector during the winter/spring is associated with the NBC retroflection, which occurs adjacent to this sector (Garzoli et al. 2003, 2004) and can disperse the particles offshore.

Monthly mean and interannual intrusion rates in the ACS were computed, revealing years of anomalously high and low intrusion. The highest monthly rates (Fig. 10[a]) of intrusion (> 10%) occurred between the months of: (i) January and March and (ii) September and October. In April, intrusion rates decreased and reached their lowest during the months of June, July and August (< 6%).

The interannual variability of particle intrusion (Fig. 10 [b]) shows an average rate of 46% ± 3%, with the lowest intrusion rates (< 43%) occurring in 2004, 2008, 2009, 2010 and 2020 and the highest rates (> 60%) in 2012, 2014 and

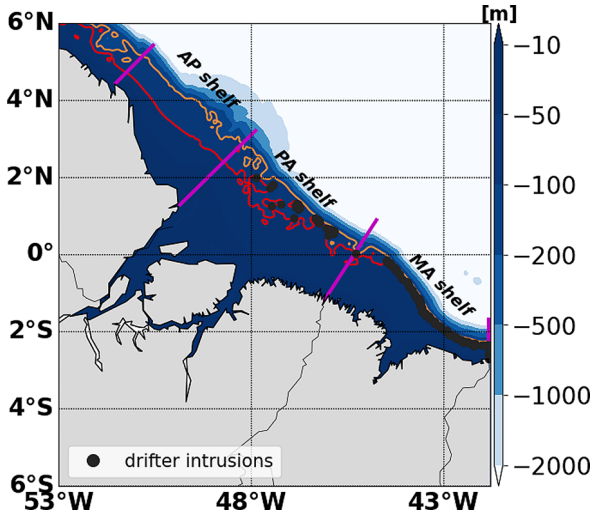

Fig. 7 Geographical location of intrusion points of the GDP drifters on the Amazon Continental Shelf (ACS). The shaded region indicates the bathymetry of the ACS, with the 50 m isobath highlighted in red, indicating the approximate middle portion of the continental shelf. The 100 m isobath is highlighted in orange, indicating the approximate position of the shelf break. The magenta lines indicate the boundaries between the sectors of the ACS

2015. No correlation was identified between annual intrusions in the ACS and the Tropical Southern Atlantic Index nor the Atlantic Meridional Mode, which are the main modes of interannual climate variability in the Equatorial Atlantic Ocean (Servain et al. 1999).

In addition to investigating the temporal variability, this study also conducted two experiments with Lagrangian modeling in order to characterize the spatial variability of the particle distribution along the ACS and adjacent oceanic region in two distinct periods of the year 2019. The relatively low interannual variability in annual particle intrusion into the ACS (Fig. 10) allows for the arbitrary selection of the year 2019, the same year that an oil spill occurred off the Brazilian coast (Soares et al. 2020). These two experiments consisted of daily release of particles in the 6 most easterly pairs of release points (Fig. 1) for 120 days, one starting in February 2019 (Fig. 11[a-d]) and the other in September 2019 (Fig. 11[e-h]). The 6 most easterly pairs of release points (Fig. 1) were chosen as these points present the highest percentage of intrusion in the ACS (Sect. 4). The periods were chosen based on the seasonality of the trade winds (Xie and Carton 2004) and the retroflection of the NBC (Garzoli et al. 2003, 2004).

Figure 11 presents a normalized particle distribution maps based on the percentage of particles that remain within the study domain after 30 [**a, e**], 60 [**b, f**], 90 [**c, g**] and 120 [**d, h**] days from the beginning of the releases (in February and September) and illustrates that although the intrusion of particles occurs in preferential sectors of the continental shelf, the particles are dispersed in all sectors of the ACS

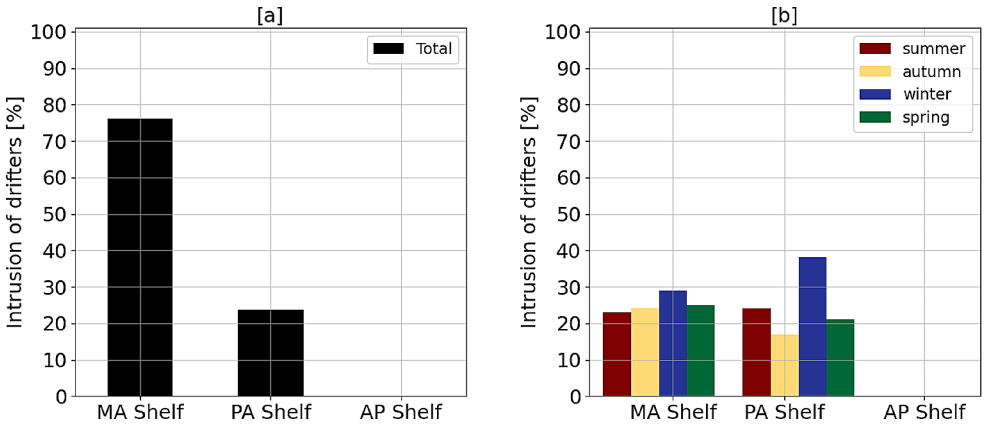

Fig. 8 Statistical characterization of the 306 GDP drifters analyzed for the study area (55°W – 40°W, 6°S to 6°N) from 2001 to 2020. The intrusion into the Amazon Continental Shelf (ACS) was observed for 122 drifters. **a** Percentage of drifters intrusion into the different sectors of the ACS. **b** Proportion of seasonal occurrence of drifter intrusions for each sector of the ACS, according to the sectors presented in Fig. 1

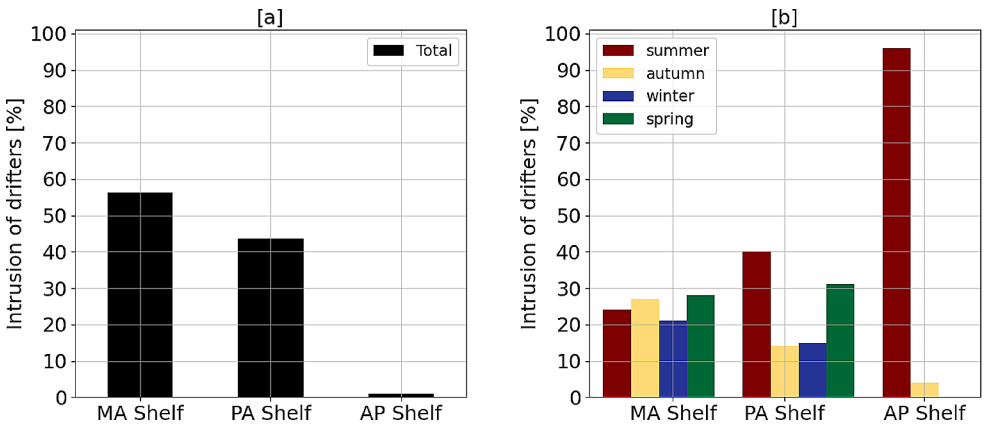

Fig. 9 Statistical analysis of 204,512 particles analysed using the Parcels toolbox in the study area (55°W – 40°W, 6°S to 6°N) from 2001 to 2020. Intrusions into the Amazon Continental Shelf (ACS) were observed in 19% of the released particles. The left panel illustrates the percentage of particle intrusions into the ACS, while the right panel displays particle intrusions categorized by season and ACS sector, as depicted in Fig. 1

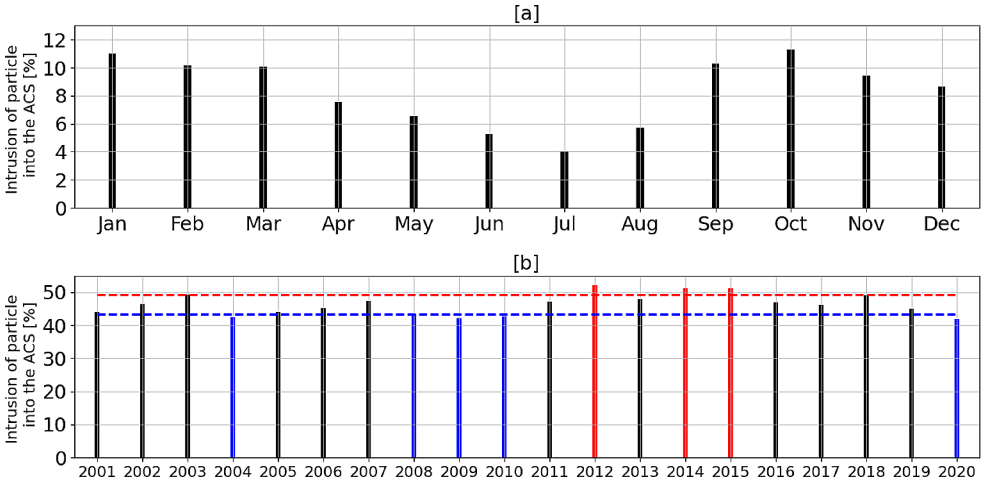

Fig. 10 Percentage of particles released by the Lagrangian model Parcels that entered the ACS per month (**a**) and per year (**b**). The red (blue) dashed line indicates the average plus (minus) one standard deviation intrusions values, in order to highlight years which had significantly more (fewer) intrusions than average

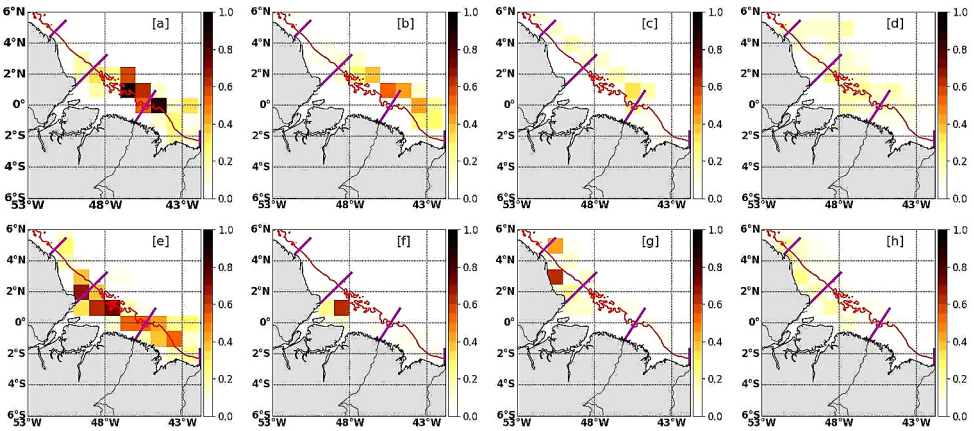

Fig. 11 Percentage map of particles based on particle launch experiments conducted with the Lagrangian Parcels toolboxfrom 393 the 6 most easterly pairs of release points (Fig. 1) in two representative periods of 2019. (a-d) The percentage of particles after 30, 394 60, 90, and 120 days of the release on February 01, 2019. (e-h) The percentage of particles after 30, 60, 90, and 120 days of the 395 release on September 01, 2019. The map domain is adjusted to focus on the distribution of particles on the continental shelf

(MA shelf, PA shelf, and AP shelf). The decrease in the number of particles during the initial 60 days of both experiments [b, f] indicates that the dispersion occurs quickly along the ACS and adjacent oceanic region. The percentage distribution of particles after the release in February [a-d] shows that particles tend to concentrate in isobaths equal to or deeper than 50 m (middle and outer shelf), while the percentage distribution of particles released in September [e-h] shows a higher concentration in isobaths equal to or shallower than 50 m (inner shelf).

In the following section, the seasonal variability of wind-driven surface circulation associated with NBC, NECC, and trade winds will be presented to discuss the patterns of drifters and particles intrusion into the ACS.

4 Discussion

The spatial variability of drifter and particle intrusion rates into the ACS (Fig. 8[a] and Fig. 9[a]) results from the combination of the continental shelf morphology and wind-driven surface circulation. The MA shelf has two morphological attributes that make it a favorable sector for surface oceanic water intrusion into the ACS: (i) the reorientation of isobaths from an E-W direction towards the NW and (ii) the proximity between the 50 and 100 m isobaths (Fig. 3). The combination of these attributes with the fact that part of the average flow of the NBC occurs close to the outer portion of the ACS (Geyer et al. 1996; Castro et al. 2006) can increase the advection of drifters onto the MA shelf. Furthermore, this explains in part the lower number of intrusions in the other sectors of the ACS, where there is a large separation between the 100 m and 50 m isobaths and relatively little changes in the orientation of the isobaths.

Furthermore, the highest percentage of particle intrusion in the MA Shelf corroborates the study of Magris et al. (2020), which showed that the coast of Maranhão was a region of the ACS heavily impacted by oil packages from a spill that occurred in an oceanic region during 2019/2020 (Soares et al. 2022). According to these authors, this spill was considered the largest in extent ever recorded in the tropical oceans. Their results are thus in accordance with ours, even though no oil spill dispersion or weathering was considered in our purely Lagrangian simulations. Both the observed drifters, Lagrangian simulations and previous studies in the region indicate that the MA Shelf sector is a preferential pathway for surface oceanic water intrusion into the ACS.

The low percentage of particle intrusion on the AP shelf can be explained by the distance between the 50 and 100 m isobaths, which indicates an average position of the NBC further away from the isobath used as the intrusion criterion in this study (50 m), and by the proximity to the retroflection region of the NBC, which has an average circulation that does not favor flows towards the continental shelf.

Figure 12 depicts the spatial variability in particle intrusion rates into the ACS from 14 pairs of release points (Fig. 1) in the Lagrangian experiment, highlighting that the higher rate (> 50%) occurs at release points located east of the MA shelf. This result corroborates the spatial intrusion pattern found in the observed data and supports the discussion about the combined effect of the morphological features of the ACS and the spatial and temporal variability of the NBC.

The seasonal (Figs. 8[b] and 9[b]) and monthly (Fig. 10[a]) variabilities in intrusion rates is a result of wind-driven surface circulation associated with the trade winds and the NBC. The mean surface velocity fields of the GLORYS (Fig. 13 [a, b]) and the wind speed at 10 m above

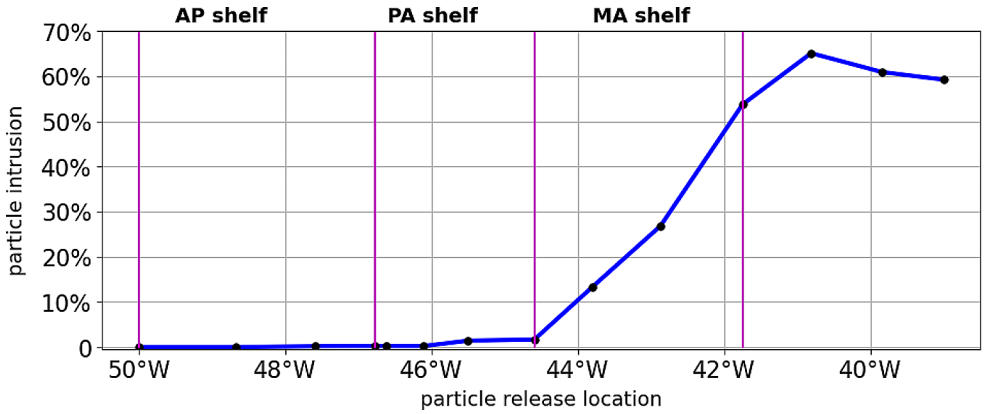

Fig. 12 Percentage of particle intrusion into the Amazon Continental Shelf from the 14 pairs of points (Fig. 1) in the Lagrangian experiment. Black dots denote the longitude of pair releases. Vertical magenta lines indicate the boundaries between the MA, PA, and AP shelves

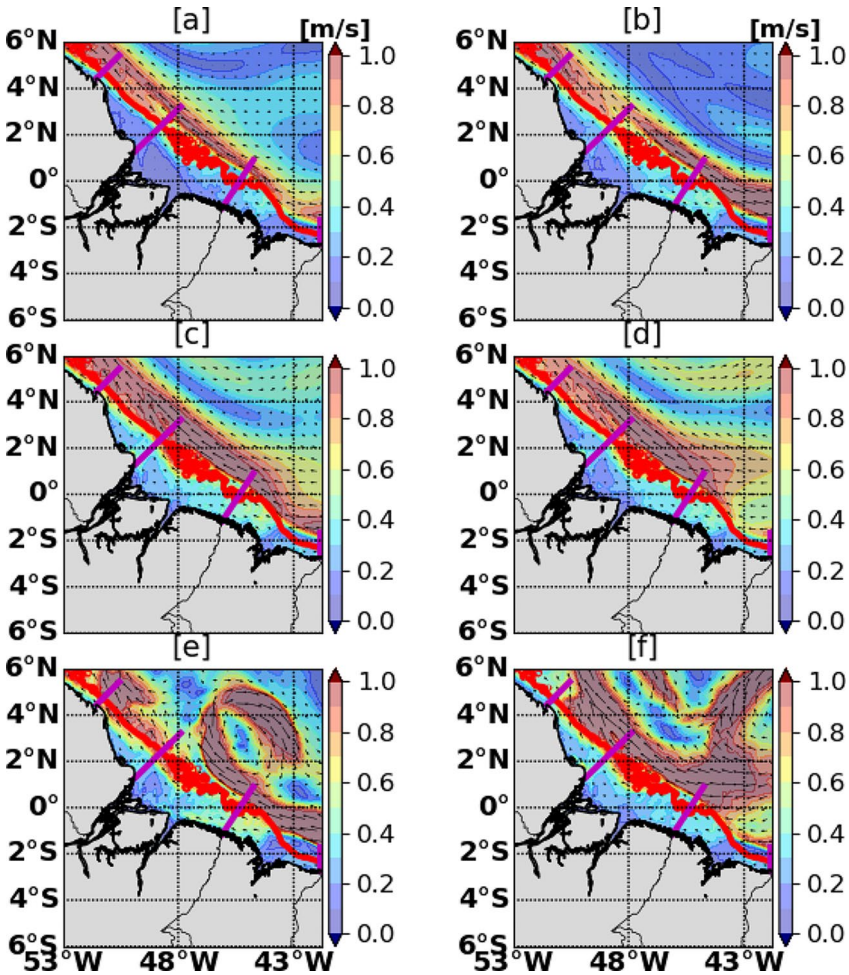

Fig. 13 Surface currents along the Equatorial Continental Margin region considering the results of 20 years (2001–2020) of simulation of the GLORYS [**a-d**]. Average circulation for the austral summer, autumn, winter and spring, respectively. [**e**] Instantaneous velocity field for June 2019 (06/01/2019) and [**f**] September 2019 (09/15/2019). The 50 m isobath is highlighted (red), indicating the approximate middle portion of the Amazon Continental Shelf. The magenta lines indicate the boundaries between the sectors of the ACS according to Fig. 1

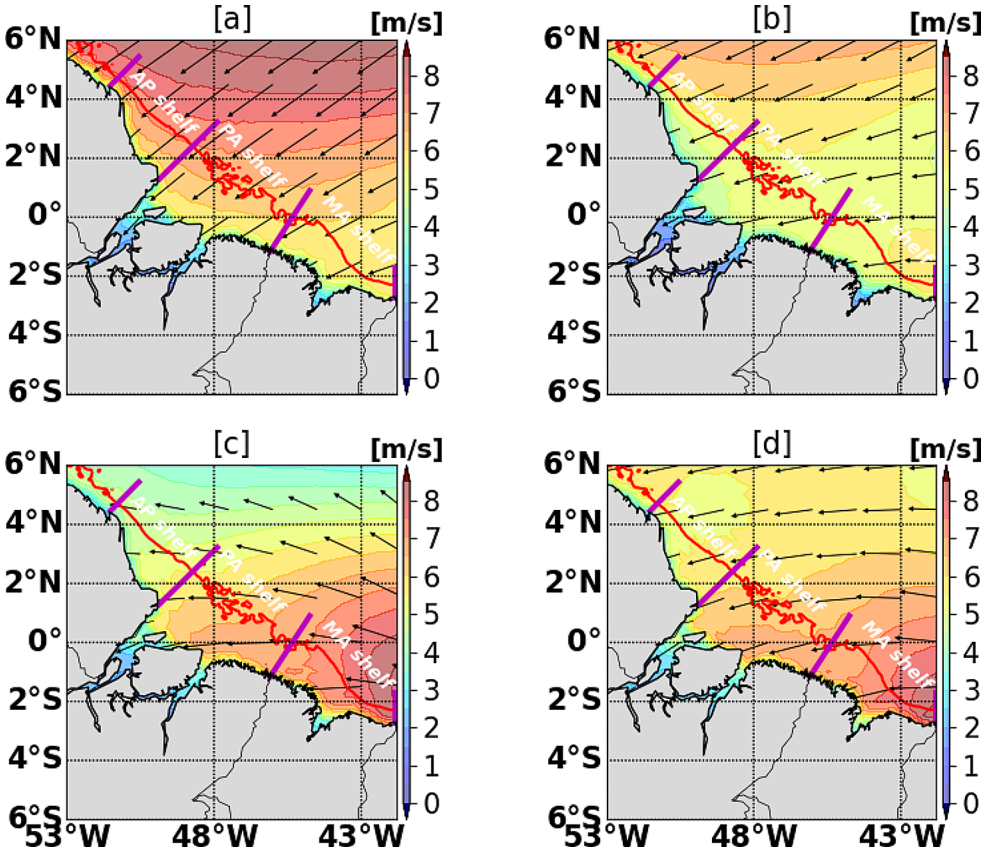

Fig. 14 Mean wind speed at 10 m height above the water surface from the ECMWF ERA5 reanalysis (2001–2020) for the austral summer [**a**], autumn [**b**], winter [**c**] and spring [**d**]. The 50 m isobath is highlighted in red, indicating the approximate middle portion of the continental shelf. The magenta lines indicate the boundaries between the sectors of the Amazon Continental Shelf according to Fig. 1

the surface from the ERA5 reanalysis (Fig. 14 [a, b]) show that during the summer and fall, the NBC exhibits a jet-like shape adjacent to the ACS, and the trade winds have a predominant direction from the northeast. These conditions are favorable for the occurrence of intrusion flows into the ACS, as observed in the data and in the Lagrangian experiments. During the winter, the NBC retroflection (Fig. 13 [c]) and the predominance of the southeast trade winds (Fig. 14 [c]) produce an average surface circulation favorable to alongshore flows, parallel to the isobaths, and of lesser potential to the generation of cross-slope transport of particles from the oceanic region to the ACS. However, it must be emphasized that the average current/wind fields are not sufficient to fully explain the intrusion processes in the ACS. Mesoscale activity plays a crucial role in intrusion rates.

The variability of ocean circulation in early winter/spring is characterized by intense mesoscale activity associated with the dynamics of the North Brazil Current/Retroflection and the North Equatorial Countercurrent (NECC) (Fonseca et al. 2004), which modulates the particle intrusion rates into the ACS. For instance, the June 2019 instantaneous velocity field (Fig. 13 [e]) illustrates hydrodynamic conditions unfavorable to particle intrusion for the PA shelf sector, because an eddy from the NBC creates an offshore flow. On the other hand, in September 2019 (Fig. 13 [f]) the mesoscale variability associated with the NBC and the NECC dynamics modulates the intensity and direction of the current field near shelf break favoring the occurrence of particle intrusion into the ACS between the MA shelf and PA shelf sectors. The mesoscale features illustrated in Fig. 13[e-f] and their respective effects on intrusion rates for ACS are recurring in the other years (2001–2020) and explain the decrease in particle intrusion observed during the months of June and July and the increase from August and September (Fig. 10 [a]). This period of minimum coincides with the beginning of the retroflection of the NBC (Schott et al. 1998) and with the predominance of southeast trade winds, mechanisms which together can cause a reduction in the intrusion of surface oceanic water into the ACS.

The distribution of particles in isobaths equal to or greater than 50 m (Fig. 11 [a-d]) may be associated with the seasonal cycle of the Amazon River discharge and the enlargement of the river plume extension along the shelf, which is wider (400–500 km) from March and May (Lentz 1995), and can modulate the dispersion of particles offshore. On the other hand, the distribution of particles in isobaths lower than 50 m (Fig. 11 [e-h]) may be the result of the combined effect of the reduction of the Amazon River discharge and the action of the trade winds (Fig. 14).

5 Conclusions

Analysis based on trajectories of GDP drifters and Lagrangian trajectories simulated by Parcels, forced by GLORYS, shows that the MA Shelf sector is the main pathway for surface ocean water intrusions into the ACS, corresponding to 56% of the intrusions, followed by PA Shelf (43%) and AP Shelf (1%). The PA and PA shelf sectors show significant seasonality in intrusion rates, higher in spring/summer for the PA shelf and in summer/autumn for the AP shelf. In contrast, the MA shelf sector shows weak seasonality in intrusion rates.

The monthly variation of intrusion rates in the ACS present minimums during June, July and August, and maximums during austral spring (October and November) and summer (February and March). The temporal variability of particle intrusion rates into the ACS is directly related to the variability of the trade winds and the circulation of the NBC and the NECC. The mesoscale activity of these currents can favor or inhibit intrusions of surface ocean waters into the continental shelf.

The percentage distribution maps of particles released in the Lagrangian simulations show that all sectors of the ACS (MA, PA, and AP Shelf) are affected during the dispersion. The seasonality of the Amazon River discharge modulates the spatial distribution of particles on the ACS, with particles concentrated in isobaths greater than or equal to 50 m during the first semester (high discharge) and in isobaths less than 50 m during the second semester (low discharge).

The complementary approach using data and Lagrangian modeling conducted in this study provided important information about the processes of oceanic surface water intrusion in the ACS. Future studies should be conducted considering subsurface water flows from the ocean to the continental shelf and the importance of internal waves as a modulating mechanism, such as internal tides.

Supplementary Information The online version contains supplementary material available at https://doi.org/10.1007/s10236-024-01606-x.

Acknowledgements The authors thank the NOAA Global Drifter Program (NOAA/AOML) for providing hourly location and current velocity collected by satellite-tracked surface drifting buoys and Copernicus Marine Environment Monitoring Service (CMEMS) for providing GLORYS results. Pedro Paulo de Freitas, Mauro Cirano and Carlos Eduardo Peres Teixeira wish to thank the Brazilian National Council for Scientific and Technological Development (CNPq) for the financial support through grants 406506/2022-1, 310902/2018-5, 315289/2021-0, respectively. Vando José Costa Gomes wish to thank the Fundação Amazônia de Amparo a Estudos e Pesquisas (FAPESPA) and the Fundação de Amparo e Desenvolvimento da Pesquisa (FADESP) for the financial support through grants 015/2019-2019/307839.

Data availability The datasets generated during and/or analyzed during the current study are available in the Global Drifter Program repository [https://www.nodc.noaa.gov/archive/arc0199/0248584/1.1/data/0-data/] and Copernicus Marine Service repository [https://data.marine.copernicus.eu/product/GLOBAL_MULTIYEAR_PHY_001_030/description].

Declarations

Conflict of interest The authors declared that they have no conflict of interest.

References

Adam O, Bischoff T, Schneider T (2016) Seasonal and interannual variations of the energy flux equator and ITCZ. Part I: Zonally averaged ITCZ position. J Clim 29(9):3219–3230. https://doi.org/10.1175/JCLI-D-15-0512.1

Aguiar AL, Marta-Almeida M, Cruz LO, Pereira J, Cirano M (2022) Forcing mechanisms of the circulation on the Brazilian equatorial Shelf. Cont Shelf Res v 247104811. https://doi.org/10.1016/j.csr.2022.104811

Almeida N, Alves M, Nepomuceno Filho TM, Freire F, Souza GSS, Oliveira ACBL, Normando KM, Barbosa MN (2020) T. H. S. A three-dimensional (3D) structural model for an oil-producing basin of the Brazilian Equatorial margin. Mar Petrol Geol 104599 https://doi.org/10.1016/j.marpetgeo.2020.104599

Araújo J, Mello Filho G, Peixoto AS, Bentes UI, Santos B, Dutka-Gianelli MAS, Isaac J, V (2022) Multidimensional evaluation of Brown Shrimp Trawling Fisheries on the Amazon Continental Shelf. Front Mar Sci 9:801758. https://doi.org/10.3389/fmars.2022.801758

Beardsley RC, Candela J, Limeburner R, Geyer WR, Lentz SJ, Castro BM, Cacchione D, Carneiro N (1995) The M2tide on the Amazon Shelf. J Phys Res 100(C2):2283. https://doi.org/10.1029/94jc01688

Berden G, Piola A, Palma R, E., D (2022) Cross-shelf Exchange in the Southwestern Atlantic Shelf: Climatology and Extreme events. Front Mar Sci 9:855183. https://doi.org/10.3389/fmars.2022.855183

Bourlès B, Gouriou Y, Chuchla R (1999) On the circulation in the upper layer of the western equatorial Atlantic. J Geophys Res Oceans v 104:21151–21170

Brink KH (2016) Cross-Shelf Exchange. Annual Rev Mar Sci, 8(1), 59–78https://doi.org/10.1146/annurev-marine-010814-015717

Castro BM, Brandini FP, Pires-Vanin AMS, Miranda LB (2006) Multidisciplinary oceanographic processes on the western Atlantic continental shelf between 4◦N and 34◦S. In: Robinson AR, Brink K (eds) The Sea - the global Coastal Ocean: Interdisciplinary Regional studies and syntheses, 14A. Harvard University Press, Harvard, USA, pp 259–293

Chen S-M (2023) Water Exchange due to wind and waves in a Monsoon Prevailing Tropical Atoll. J Mar Sci Eng 11:109. https://doi.org/10.3390/jmse11010109

Coles VJ, Brooks MT, Hopkins J, Stukel MR, Yager PL, Hood RR (2013) The pathways and properties of the Amazon River Plume in the tropical North Atlantic Ocean. J Geophys Res Oceans 118:6894–6913. https://doi.org/10.1002/2013JC008981

Combes V, Matano RP, Palma ED (2021) Circulation and cross-shelf exchanges in the northern shelf region of the southwestern Atlantic: kinematics. J Geophys Research: Oceans., 126, e2020JC016959 https://doi.org/10.1029/2020JC016959

Cruz R, Cintra IHA, Silva KCA, Abrunhosa FA (2013) Structure and diversity of the lobster community on the Amazon

continental shelf. Crustaceana 86(9):1084–1102. https://doi.org/10.1163/15685403-00003227

Cruz CA, Ribeiro S, H. J. P., da Silva EB (2021) Exploratory plays of the Foz do Amazonas Basin, NW portion, in deep and ultra-deep waters. Brazilian Equatorial Margin J South Am Earth Sci 111:103475. https://doi.org/10.1016/j.jsames.2021.103475

Dee DP, Uppala SM, Simmons AJ, Berrisford P, Poli P, Kobayashi S, Andrae U, Balmaseda MA, Balsamo G, Bauer P, Bechtold P, Beljaars ACM, van deBerg L, Bidlot J, Bormann N, Delsol C, Dragani R, Fuentes M, Geer AJ, Haimberger L, Healy SB, Hersbach H, ́olm H, Isaksen EV, ̊allberg LK P., McNally M, Monge-Sanz AP, Morcrette BM, Park J-J, Peubey B-K, de Rosnay C, Tavolato P, Thépaut C, Vitart J-N F (2011) The ERA-Interim reanalysis: configuration and performance of the data assimilation system. Q J R Meteorol Soc 137:553–597 K ̈ohler M.,Matricardi. https://doi.org/10.1002/qj.828

Delandmeter P, van Sebille E (2019) The parcels v2.0 Lagrangian framework: new field interpolation schemes. Geosci Model Dev 12:3571–3584. https://doi.org/10.5194/gmd-12-3571-2019

Elipot S, Lumpkin R, Perez R, Lilly C, Early JM, Sykulski JJ, A., M (2016) A global surface drifter data set at hourly resolution. J Geophys Res Oceans 121:2937–2966. https://doi.org/10.1002/2016JC011716

Elipot S, Sykulski A, Lumpkin R, Centurioni L, Pazos M (2022) Hourly location, current velocity, and temperature collected from global drifter program drifters world-wide. https://doi.org/10.25921/x46c-3620. NOAA National Centers for Environmental Information. Dataset

Fonseca C, Goni A, Johns GJ, Campos WE, E., J., D (2004) Investigation of the North Brazil current retroflection and north equatorial countercurrent variability. Geophys Res Lett v 31:L21304. https://doi.org/10.1029/2004GL020054

Fontes RFC, Castro BM, Beardsley RC (2008) Numerical study of circulation on the inner Amazon Shelf. Ocean Dyn 58(3–4):187–198. https://doi.org/10.1007/s10236-008-0139-4

Francini-Filho R, Asp N, Siegle E, Hocevar J, Lowyck K, D'Avila N, Vasconcelos A, Baitelo A, Rezende R, Omachi CE, Thompson CY, Thompson CC, F. L (2018) Perspectives on the great amazon reef: extension. Biodiversity and threats. Front Mar Sci 5:142. https://doi.org/10.3389/fmars.2018.00142

Garcia TM, Campos CC, Mota EMT, Santos NMO, Campelo RP, de Prado S, Junior LCG, de Soares MM O (2020) Microplastics Subsurface Waters Western Equatorial Atl (Brazil) Mar Pollution Bull 110705. https://doi.org/10.1016/j.marpolbul.2019.110705

Garzoli SL, Ffield A, Yao Q (2003) NBC retroflection and rings, in Interhemispheric Water Exchange in the Atlantic Ocean, Elsevier Oceanogr. Ser., vol. 68, edited by G. Goni, and P. Malanotte-Rizzoli, pp. 357 – 374, Elsevier Sci., New York

Garzoli S, Ffield L, Johns A, Yao WE, Q (2004) North Brazil current retroflection and transports. J Phys Res 109:C01013. https://doi.org/10.1029/2003JC001775

Geyer WR, Beardsley RC, Lentz SJ, Candela J, Limeburner R, Johns WE, Castro B, Soares M (1996) I., D. Physical oceanography of the Amazon shelf. Continental Shelf Res 16(5–6), 575–616 https://doi.org/10.1016/0278-4343(95)00051-8

Guerrero L, Sheinbaum J, Mariño-Tapia I, Gonzalez-Rejón J J., Pérez-Brunius P (2020) Influence of mesoscale eddies on cross-shelf exchange in the western Gulf of Mexico. Cont Shelf Res 209:104243. https://doi.org/10.1016/j.csr.2020.104243

Huang G, Zhan H, He Q, Wei X, Li B (2021) A lagrangian study of the near-surface intrusion of Pacific water into the South China Sea. Acta Oceanol Sin 40(7):15–30. https://doi.org/10.1007/s13131-021-1766-6

Huthnance J (1995) M., Circulation, exchange and water masses at the ocean margin: the role of physical processes at the shelf edge. Prog Oceanogr 35(4), 353–431 https://doi.org/10.1016/0079-6611(95)80003-c

Huthnance J, Hopkins J, Berx B, Dale A, Holt J, Hosegood P, Inall M, Jones S, Loveday B, Miller R, Polton PI, Porter J, Spingys M, C (2022) Ocean shelf exchange, NW European shelf seas: measurements, estimates and comparisons. Prog Oceanogr 202:102760. https://doi.org/10.1016/j.pocean.2022.102760

Iskandar MR, Cordova MR, Park Y-G (2022) Pathways and destinations of floating marine plastic debris from 10 major rivers in Java and Bali, Indonesia: a lagrangian particle tracking perspective. Mar Pollut Bull 185:114331. https://doi.org/10.1016/j.marpolbul.2022.114331

Jean-Michel L, Eric G, Romain Bé-B, Gilles G, Angélique M, Marie D, Clément B, Mathieu H, Olivier LG, Charly R, Tony C, Charles-Emmanuel T, Florent G, Giovanni R, Mounir B, Yann D, Pierre-Yves LT (2021) The Copernicus Global 1/12° Oceanic and Sea Ice GLORYS12 reanalysis. Front Earth Sci 9:698876. https://doi.org/10.3389/feart.2021.698876

Johns WE, Lee TN, Beardsley RC, Candela J, Limeburner R, Castro B (1998) Annual Cycle and Variability of the North Brazil Current. Journal of Physical Oceanography, 28(1), 103–128 https://doi.org/10.1175/1520-0485(1998)028<0103:ACAVOT>2.0.CO;2

Lavagnino AC, Bastos AC, Filho A, de Moraes GM, Araujo FC, de Moura LS, R. L (2020) Geomorphometric seabed classification and potential Megahabitat distribution in the Amazon Continental Margin. Front Mar Sci 7:190. https://doi.org/10.3389/fmars.2020.00190

Lellouche J-M, Greiner E, Le Galloudec O, Garric G, Regnier C, Drevillon M et al (2018) Recent updates to the Copernicus Marine Service Global Ocean Monitoring and forecasting real-time 1/12 ° high-resolution system. Ocean Sci 14:1093–1126. https://doi.org/10.5194/os-14-1093-2018

Lentz SJ (1995) Seasonal variations in the horizontal structure of the Amazon Plume inferred from historical hydrographic data. J Geophys Res 100(C2), 2391–2400 https://doi.org/10.1029/94jc01847

Lentz SJ, Limeburner R (1995) The Amazon River Plume during AMASSEDS: Spatial characteristics and salinity variability. J Geophys Res 100(C2), 2355–2375 https://doi.org/10.1029/94jc01411

Lessa GC, Teixeira CEP, Pereira J, Santos FM (2021) The 2019 Brazilian oil spill: insights on the physics behind the drift. J Mar Syst 222:103586. https://doi.org/10.1016/j.jmarsys.2021.103586

Louchard D, Gruber N, Münnich M (2021) The impact of the Amazon on the biological pump and the air-sea CO_2 balance of the Western Tropical Atlantic. Glob Biogeochem Cycles 35. https://doi.org/10.1029/2020GB006818

Madec G, the NEMO Team (2008) NEMO Ocean Engine. Note Du Pôle De modélisation, vol 27. Institut Pierre-Simon Laplace (IPSL), France, pp 1288–1619

Magris RA, Giarrizzo T (2020) Mysterious oil spill in the Atlantic Ocean threatens marine biodiversity and local people in Brazil. Mar Pollut Bull v 153:110961. https://doi.org/10.1016/j.marpolbul.2020.110961

Malan N, Archer M, Roughan M, Cetina-Heredia P, Hemming M, Rocha C, Schaeffer A, Suthers I, Queiroz E (2020) Eddy-driven cross-shelf transport in the East Australian Current separation zone. J Geophys Res Oceans 125, e2019JC015613 https://doi.org/10.1029/2019JC015613

Matano RP, Combes V, Piola AR, Guerrero R, Palma ED, Ted Strub P, James C, Fenco H, Chao Y, Saraceno M (2014) The salinity signature of the cross-shelf exchanges in the Southwestern Atlantic Ocean: Numerical simulations. J Geophys Res Oceans 119(11):7949–7968. https://doi.org/10.1002/2014jc010116

Molinas E, Carneiro JC, Vinzon S (2020) Internal tides as a major process in Amazon continental shelf fine sediment transport. Mar Geol 430:106360. https://doi.org/10.1016/j.margeo.2020.106360

Moura RL, Amado-filho GM, Moraes FC, Brassileiro PS, Salomon PS, Mahiques MM et al (2016) An extensive reef system at the Amazon River mouth. Sci Adv 2:1–12. https://doi.org/10.1126/sciadv.1501252

Nittrouer CA, DeMaster DJ (1986) Sedimentary processes on the Amazon continental shelf: past, present and future research. Continental Shelf Res 6(1–2), 5–30 https://doi.org/10.1016/0278-4343(86)90051

Nittrouer C, DeMaster A (1996) D J The Amazon shelf setting: tropicnergetic, and influenced by a large river. Cont Shelf Res 16 5-6 553–573 https://doi.org/10.1016/0278-4343(95)00069-0

Oliveira J, Aguiar C, Cirano W, Genz M, F., de Amorim FN (2018) A climatology of the annual cycle of river discharges into the Brazilian continental shelves: from seasonal to interannual variability. Environ Earth Sci 77(5). https://doi.org/10.1007/s12665-018-7349-y

Prestes YO, Silva AC, Jeandel C (2018) Amazon water lenses and the influence of the North Brazil Current on the continental shelf. Cont Shelf Res 160:36–48

Schneider T, Bischoff T, Haug GH (2014) Migrations and dynamics of the intertropical convergence zone. Nature 513(7516), 45–53 https://doi.org/10.1038/nature13636

Schott FA, Stramma L, Fischer J (1995) The warm water inflow into the western tropical Atlantic boundary regime, 1994, J Geophys Res 400, 24,745–24,760

Schott FA, Fischer J, Stramma L (1998) Transports and pathways of the Upper-Layer circulation in the Western Tropical Atlantic. J Phys Oceanogr v 28:1904–1928

Schott FA, Dengler M, Zantopp R, Stramma L, Fischer J, Brandt P (2005) The shallow and deep western boundary circulation of the South Atlantic at 5°–11°S. J Phys Oceanogr v 35(11):2031–2053

Servain J, Wainer I, McCreary Jr J, Dessier P, A (1999) Relationship between the equatorial and meridional modes of climatic variability in the tropical Atlantic. 26(4):485–488. Geophysical Research Letters10.1029/1999GL900014

Silva AC, Araújo M, Bourlès B (2005) Variação Sazonal Da estrutura de massas de água na plataforma continental do Amazonas E área oceânica adjacente. Rev Brasileira Geofís 23(2):145–157. https://doi.org/10.1590/S0102-261X2005000200004

Silveira ICA, Miranda LB, Brown WS (1994) On the origins of the North Brazil Current. J Geophys Res v 99:22501–22512

Silveira ICA, Bernardo PS, Lazaneo CZ, Amorim JPM, Borges-Silva M, Martins RC, Santos DMC, Dottori M, Belo WC, Martins RP, Guerra LAA, Moreira DL (2023) Oceanographic conditions of the continental slope and deep waters in Santos Basin: the SANSED cruise (winter 2019). Ocean Coastal Res 71:e23008. https://doi.org/10.1590/2675-2824071.2206icas

Soares MO, Teixeira CEP, Bezerra LEA, Paiva SV, Tavares TCL, Garcia TM, Araújo JT, Campos CC, Ferreira SMC, Matthews-Cascon H, Frota A, Mont'alverne TCF, Silva ST, Rabelo EF, Barroso CX, Freitas JEP, Júnior MM, Santana Campelo RP, Santana CS, Macedo Carneiro PB, Meirelles AJ, Santos BA, Oliveira AHB, Horta P, Cavalcante RM (2020) Oil spill in South Atlantic (Brazil): environmental and governmental disaster. Mar Policy 115:103879. https://doi.org/10.1016/j.marpol.2020.103879

Soares MO, Teixeira CEP, Bezerra LEA et al (2022) The most extensive oil spill registered in tropical oceans (Brazil): the balance sheet of a disaster. Environ Sci Pollut Res 29:19869–19877. https://doi.org/10.1007/s11356-022-18710-4

Stramma L, Rhein M, Brandt P, Dengler M, Böning C, Walter M (2005) Upper ocean circulation in the western tropical Atlantic in boreal fall 2000. 52(2):221–240Deep Sea Research Part I: Oceanographic Research Papers, v

Xie S-P, Carton JA (2004) Tropical Atlantic variability: patterns, mechanisms, and impacts. In: Wang C, Xie S-P, Carton JA (eds) Earth Climate: The Ocean-Atmosphere Interaction. Am. Geophys. Union, Washington DC, pp 121–142

Zhou F, Xue H, Huang D, Xuan J, Ni X, Xiu P, Hao Q (2015) Cross-shelf exchange in the shelf of the East China Sea. J Geophys Res Oceans 120:1545–1572. https://doi.org/10.1002/2014JC010567